

<https://doi.org/10.1038/s42003-025-08082-z>

Emergence of a synergistic scaffold in the brains of human infants

Check for updates

Thomas F. Varley^{1,2,3,9}, Olaf Sporns^{1,9}, Nathan J. Stevenson⁴, Pauliina Yrjölä^{5,6}, Martha G. Welch⁷, Michael M. Myers⁷, Sampsa Vanhatalo^{5,6} & Anton Tokariev^{1,6,8,9}✉

The human brain is a complex organ comprising billions of interconnected neurons, which enables interaction with both physical and social environments. Neural dynamics of the whole brain go far beyond just the sum of its individual elements; a property known as “synergy”. Previously it has been shown that synergy is crucial for many complex brain functions and cognition, however, it remains unknown how and when the large number of discrete neurons evolve into the unified system able to support synergistic interactions. Here we analyzed high-density electroencephalography data from the late fetal period to one month after term age. We found that the human brain transitions from a redundancy-dominated to a synergy-dominated system around birth. Frontal regions lead the emergence of a synergistic scaffold comprised of overlapping subsystems, while the integration of sensory areas developed gradually, from occipital to central regions. Strikingly, early developmental trajectories of brain synergy were modulated by environmental enrichment associated with enhanced mother-infant interactions, and the level of synergy near term equivalent age was associated with later neurocognitive development.

The human brain is a paradigmatic example of a complex system displaying emergent structure. Despite being composed of billions of individually functioning neurons, their collective dynamics lead to the emergence of a unified “whole” capable of integrating information, learning, and surviving in complex environments. The property, where a system collectively shows structure that is irreducible to the sum of its parts, is known as synergy¹, and it is thought to play a key role in the self-organization of the brain into a unified whole^{2,3}. Understanding this process is a fundamental challenge in modern neuroscience. Information theory has emerged as a core toolkit for the analysis of modern complex systems science⁴, and has been used to explore the structure of information processing and cognition in the brain at multiple scales^{5–7}. Previous fMRI studies on adults have shown that synergistic sub-systems are widespread across the cortex^{7,8}, and that the distribution of synergies changes across the adult lifespan⁵.

In the development of an individual's brain, functional synergy can only emerge after the development of underlying structural brain networks. It is currently well established that most structural and functional organization in brain networks takes place during the few months around birth^{9–14}.

This process is driven by a combination of genetically guided growth of the major structural networks and an activity-dependent organization of the functional networks^{15–18} into integrated and segregated ensembles that together form the synergistic whole^{2,19}. However, it is not known how and when synergistic brain function appears, and whether it emerges sequentially or uniformly across the newly developed cortex. Spontaneous cortical activity in large neuronal ensembles directly facilitates the emergence of the brain's functional synergistic structure. Recording this activity provides a natural test-bed to study the self-organization of higher-order dependencies in the brain. In this paper, we use information theory to assess the emergence of a “synergistic scaffold” in the functional architecture of the brain from the late fetal period to one month after term age.

We hypothesized that synergy emerges in spatially resolved sequences during the early development of the brain, and, moreover, that the emergence of a consolidated “synergistic scaffold” links to later neurocognitive performance at individual level. To test this, we used a recently proposed measure of higher-order structure in complex systems: the O-Information (Ω)²⁰. The O-information can assess whether the statistical structure of a

¹Department of Psychological and Brain Sciences, Indiana University Bloomington, Bloomington, IN, 47408, USA. ²School of Informatics, Computing, and Engineering, Indiana University Bloomington, Bloomington, IN, 47408, USA. ³Vermont Complex Systems Center, University of Vermont, Burlington, VT, 05405, USA. ⁴Brain Modelling Group, QIMR Berghofer Medical Research Institute, Brisbane, QLD, 4006, Australia. ⁵BABA Center, Pediatric Research Center, Department of Clinical Neurophysiology, New Children's Hospital, Helsinki University Central Hospital, 00029 Helsinki, Finland. ⁶Department of Physiology, University of Helsinki, 00014 Helsinki, Finland. ⁷Departments of Psychiatry and Pediatrics, Columbia University Medical Center, New York, NY, 10032, USA. ⁸Early Brain Activity, Systems, and Health Group, University of Helsinki, 00014 Helsinki, Finland. ⁹These authors contributed equally: Thomas F. Varley, Olaf Sporns, Anton Tokariev.

✉ e-mail: anton.tokariev@helsinki.fi

complex system, such as global EEG activity, is synergy-dominated (i.e., the collective whole contains information that is irreducible to smaller collections of parts) or redundancy-dominated (i.e., the collective whole can be compressed or simplified by pruning duplicated information). For a given multivariate system \mathbf{X} , if $\Omega(\mathbf{X}) < 0$, then the system is synergy dominated, and if $\Omega(\mathbf{X}) > 0$, then the system is redundancy dominated. In this study, we determined the level and topographic distribution of O-information during early development of spontaneous cortical activity in newborn infants. First, we estimated the O-information across the whole brain to assess global information structure in the EEG. Second, we extracted maximally synergistic subsystems to identify regional subsets with the highest synergy. This yielded spatially resolved tracking of the emerging synergistic subsystems in fine-grained detail, which could then be compared to functional hierarchies and later neurocognitive development.

Results

We collected 124-channel sleep EEG recordings from 136 preterm infants (born at 31 ± 2.4 weeks gestational age) longitudinally during the third trimester, between 33 and 45 postnatal weeks (see Supplementary Fig. S1). Next, 5-min-long epochs of quiet ($N = 289$) and active ($N = 301$) sleep were classified, source reconstructed into 58 cortical parcels using an infant head model, and filtered into four frequency bands of interest: delta (1.5–4 Hz), theta (4–8 Hz), alpha (8–13 Hz), and beta (13–22 Hz). Cortical signals were used to compute O-information that reflects the balance between synergy and redundancy in the system. For each recording we also identified the subset of regions which comprise the most synergy in the brain (synergistic scaffolds). These data were used to study the developmental changes of the global O-information and the build-up of the synergistic scaffold. To define the link to neurodevelopment, we correlated the levels of synergy in the brain around term age to Bayley cognitive scores of the same infants at 18 months. Finally, we split the general group into two clinical subgroups: standard care (SC, $N = 62$) and family nurture intervention (FNI, $N = 74$) infants to compare their developmental trajectories in terms of synergistic organization of the brain. For these groups we also compared the functional maturation of cortical regions over the same period.

Synergy in the brain increases during early maturation

We found that O-information becomes increasingly negative with age at all studied frequency bands in quiet sleep (Fig. 1A; $\rho < -0.42$, $p\text{FDR} < 0.001$, Spearman test), indicating a transition from a redundancy-dominated to a synergy-dominated structure. The effect size was the strongest at higher frequencies (alpha, 8–13 Hz, $\rho = -0.57$; and beta, 13–22 Hz, $\rho = -0.59$). These preterm infants, when assessed at postconceptional ages less than term age, showed high positive O-information values suggesting a prevalence of redundancy-dominated dynamics, while the O-information levels shifted towards zero and even became negative around term age. Analysis of active sleep EEG also revealed similar robust trends across all frequencies (Supplementary Fig. S2; $\rho < -0.31$, $p\text{FDR} < 0.001$). Once again reflecting increasing presence of synergy, and the transformation of the brain into a more synergy-dominated system. These results are similar to prior works demonstrating changes in connectivity networks in the preterm brain during early development^{21,22}, and future work focused on assessing the underlying common drivers of these changes is warranted. Assessing the strength (O-information) of the most synergistic ensembles of brain regions, across all possible subsystem sizes (i.e., the number of brain regions in an ensemble), in individual infants (Fig. 1B, top row) revealed systematic increases in negative O-information across all temporal scales as a function of age. At the same time, the number of brain regions in the optimal system (or “synergistic subsystem”) grew at an accelerated pace near term age (Fig. 1B, bottom row). In Fig. 1B, this is represented by the global minima of the curves drifting down and to the right, indicating lower optimal O-information (more synergy-dominance) and larger systems sizes. We also found that expansion of the “synergistic subsystem” across the whole cortex and increase of the overall synergy are two highly correlated signatures of early brain development (Fig. 1C; $\rho < -0.65$, $p\text{FDR} < 0.001$ for all, Spearman test).

The synergistic scaffold expands sequentially from the frontal to other brain regions

Next, we analyzed the early development of the spatial configuration of the “synergistic scaffold” by comparing nodal participation frequency in three age groups: early preterm (33–36 weeks), late preterm (37–40 weeks), and after normal full term age (40–43 weeks). These maps indicate participation frequency of the given cortical region (or “node”) in the synergistic scaffold (Fig. 2). We used binomial statistics to test whether nodes belonging to distinct anatomical regions (frontal, central, occipital, or temporal) were significantly overrepresented in each scaffold. Specifically, we compared the observed frequency of nodes from each category in the scaffold to their expected probability at the group level. In the early preterm infants (Fig. 2, top row), the synergistic scaffold was dominated by a symmetric frontal cluster ($p < 0.0001$, for all frequencies), and a markedly less prominent occipital cluster that was robustly present only at beta frequencies (13–22 Hz; $p = 0.01$). In comparison, the late preterm group showed spatial expansion and an increase in participation frequency across subjects for the frontal ($p < 0.0001$) and occipital ($p \leq 0.04$) clusters in a whole frequency range (Fig. 2, middle row). In the after-term age group, the synergistic scaffold had expanded considerably to include the central cortical areas as well (Fig. 2, bottom row). However, while nodes of fronto-occipital axis were robustly present in the scaffold at all frequencies ($p < 0.0001$), the presence of other regions were less consistent yet (not significant on the group level). Overall, this sequential recruitment of cortical areas is consistent with recent studies in adults that found that high-synergy systems tended to straddle multiple canonical functional networks^{7,19}. Unthresholded maps of the developmental changes in the synergistic scaffold are shown in Supplementary Fig. S3.

Newborn brain synergy precedes long-term neurocognitive development

We then asked if the level of synergy at the time of normal birth has neurodevelopmental implications. To this end, we correlated O-information metrics taken around term age (38–42 weeks) with later neurocognitive performance assessed at 18 months using standardized Bayley Scales (available for $N = 41$ subjects^{23,24}). We used the Bayley Cognitive Scale, which assesses early cognitive skills such as attention, memory, problem-solving, and sensory processing (see section ‘Association with neurodevelopment’ for more details). Three subjects out of this sample had two recordings corresponding to this period, thus for them we used mean O-information values. The later neurocognition was robustly correlated to the individual O-information levels across the whole frequency range of interest (Fig. 3A; $\rho < -0.41$, $p\text{FDR} < 0.008$). These correlations were not affected after regressing age at EEG recording from the O-information values (see bottom row on Fig. 3A). Other characteristics of synergistic subsystems were also linked to later neurocognitive development. The minimum O-information showed negative correlation with later performance (Fig. 3B, top row; $\rho < -0.32$, $p\text{FDR} < 0.039$), suggesting that the early emergence of synergistic structures may promote cognitive development. Similarly, the number of brain regions in the optimal synergistic subsystem was strongly correlated with better cognitive performance (Fig. 3B, bottom row; $\rho \geq 0.46$, $p\text{FDR} < 0.002$), suggesting that later cognitive development may benefit from including wider brain areas in the synergistic whole. Taken together, our results suggest that the level of overall synergistic cortical activity during quiet sleep, as well as its spatial expansion over the cortex strongly reflect an individual’s capacity for neurocognitive development. During active sleep, O-information also negatively correlated to cognitive scores but did not reach statistical significance ($-0.25 < \rho < -0.18$, $0.11 < p < 0.23$, for all frequencies).

Environmental enrichment modulates early developmental trajectories of brain synergy

Intertwined with the genetically predefined schedules of brain development^{25,26}, there is growing evidence that early activity-dependent brain development can be substantially affected by environmental

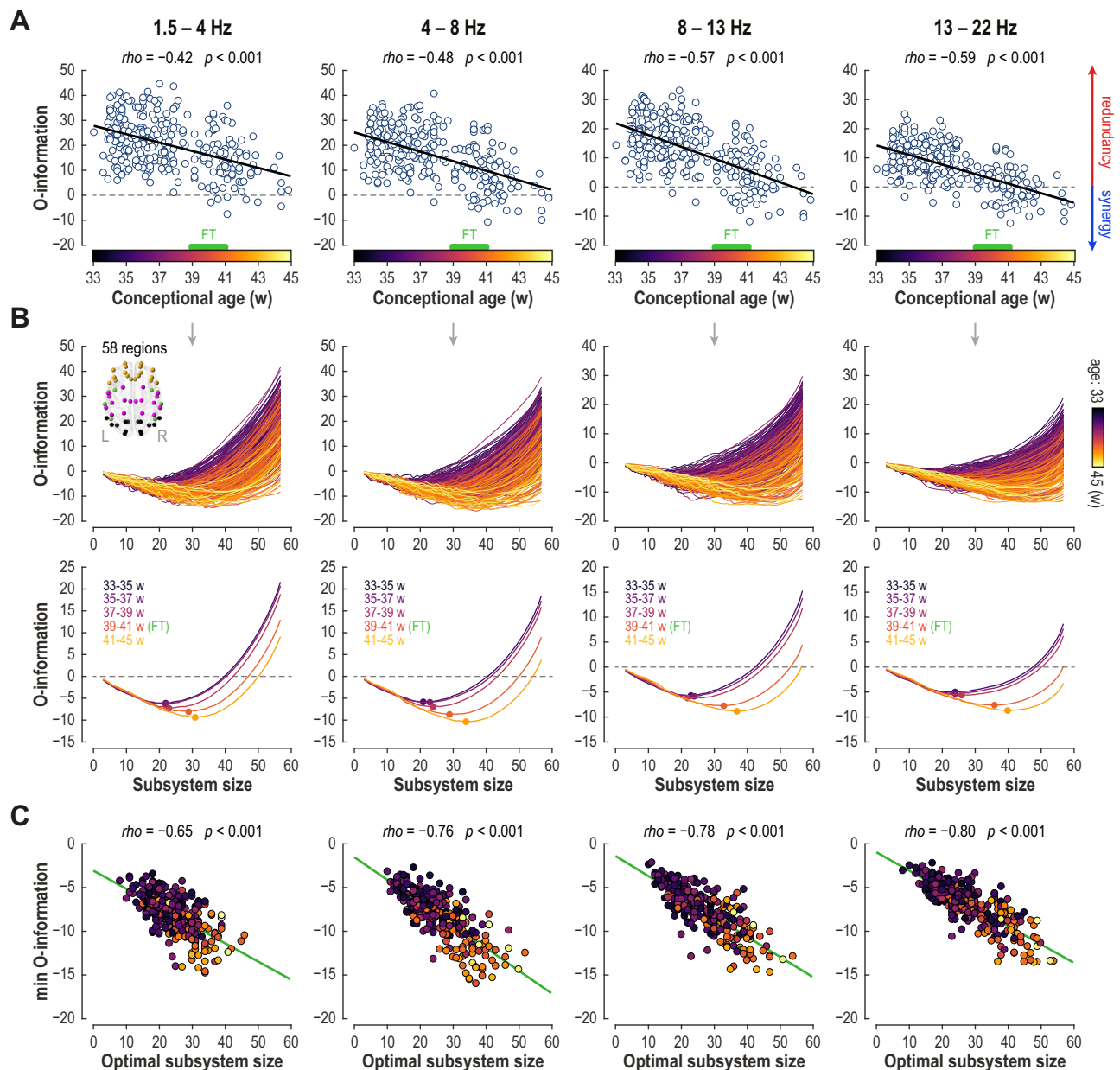


Fig. 1 | Emergence of synergistic brain during the three months around birth.

A The global values of the O-information become significantly more negative at all inspected oscillatory frequencies (Spearman) pointing to emerging synergy towards full term (FT) age. **B** Relationship between optimally synergistic O-information and the subsystem size (i.e., number of included brain regions) in individual infants (top row) and in averaged age groups (bottom row), colored for the infant's age at EEG recording. The dots in the bottom plots depict the minimum of O-information curves that reflects the size of subsystems with maximum synergy in the given age group (the optimal “synergistic subsystem”). Note, the systematic growth of the synergistic subsystem with age at all frequencies (optimal system size vs. age:

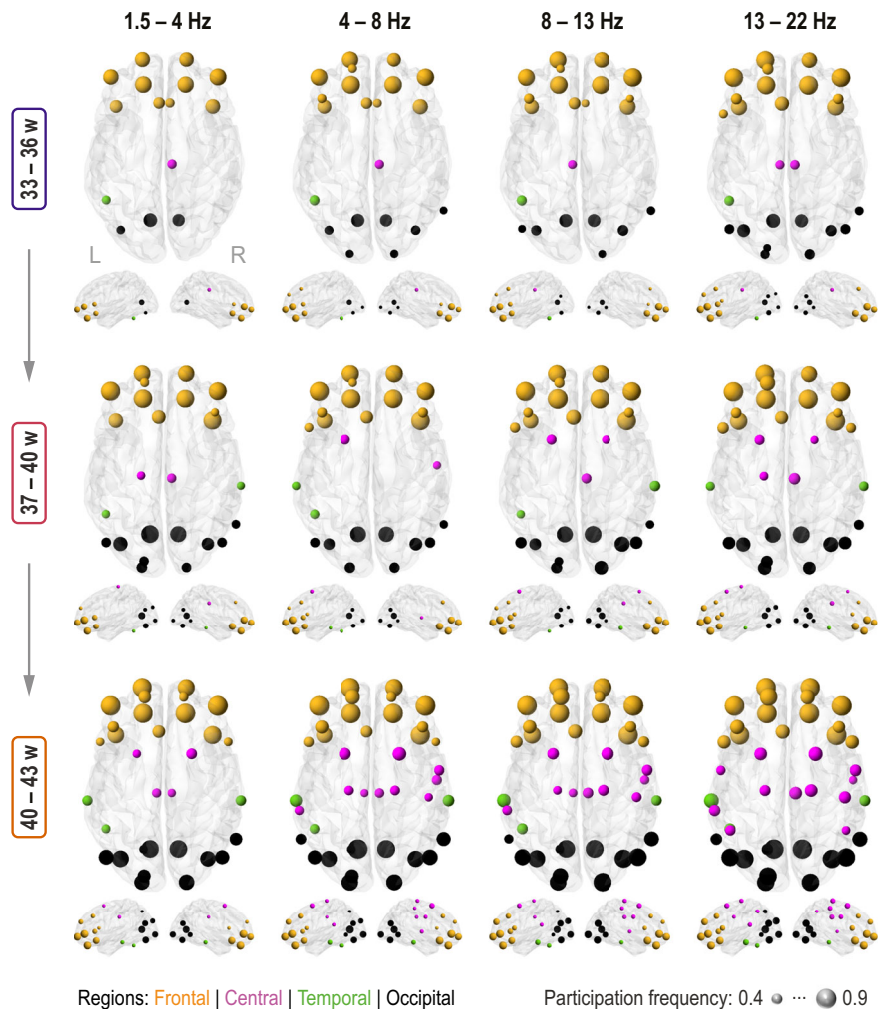
$\rho > 0.44$, $p < 0.001$, Spearman), with particularly rapid changes around term age. The glass brain shows all cortical regions (full system) that are color coded according to their anatomical location: frontal (orange), central (magenta), temporal (green), and occipital (black). To find the individual synergistic scaffolds, all possible subsets of nodes (from 3 to 57) were tested. **C** Relationship (Spearman) between O-information levels and the size of the maximally synergistic subsystem in individual EEG (computed from the curves on the top row in (B); colors code the age at recording). Developmental expansion of the synergistic subsystem and increase of its synergistic capacity are highly correlated (the brain becomes more complex).

factors^{16,18,27–30}. These “acquired effects” range from major medical adversities like preterm birth or perinatal asphyxia^{31–34} to more subtle issues^{29,35–37}. Recent preclinical and clinical studies have suggested that various changes in an infants’ living environment (“environmental enrichments”) may support improved neurodevelopment at many levels of inspection from the cellular level³⁸ to brain networks^{22,39,40}, brain structure⁴¹, and many aspects of later neurobehavioural outcomes^{24,42}. Therefore, we assessed whether the early emergence of synergistic brain activity could be affected by the living environment. To this end, we took advantage of having two subgroups in our dataset: half of the infants had been treated according to all the evidence-

based guidelines of preterm care (standard care group, SC); the other half was assigned to a group that received additional intervention during their stay in the neonatal intensive care unit to facilitate emotional parent-infant connection (Family Nurture Intervention, FNI;⁴³ which is considered to be biologically relevant, and also a natural part of an optimal nursing practice^{43–46}.

The developmental trajectories of O-information, computed using two-weeks-wide sliding time windows with 50% overlap, were clearly different between these subgroups (Wilcoxon rank-sum test; Fig. 4A). The SC infants showed a bi-phasic trajectory with an initial plateau (corresponding

Fig. 2 | Early spatial development of the synergistic scaffold at different frequency bands. The ball size indicates participation frequency, of each cortical region (“node”) in the optimally synergistic ensembles (collectively forming the “synergistic scaffold”) in different age groups (rows), and at different frequency bands (columns). For each infant, maximally synergistic subsets of the whole brain were discovered using simulated annealing¹²², with the negative O-information as the objective function (for details see “Materials and methods”). Running the optimizer a large number of times reveals a landscape of non-identical, but overlapping, synergistic ensembles, which recruit brain regions from different areas at distinct periods of development, so we extracted the number of times each node was selected across all trials of all infants, and visualize¹²⁵ those that appear in > 40% of optimal sets. Note the early prominence of frontal synergistic scaffold, the incremental recruitment of the occipital regions, and the late-appearing participation of the central regions. The colors indicate the anatomical affiliation in different cortical regions: frontal (orange), central (purple), temporal (green), and occipital (black).



to a maximum of redundancy) until near term age (≈ 38 weeks) followed by an abrupt transition towards greater synergy, whereas the FNI infants showed a steady increase in synergy (i.e. decrease of O-information). The groups were consistently different across all frequencies at two time points: 35 weeks (FNI > SC; $p < 0.051$ for all); and 38 weeks (FNI < SC; $p < 0.033$ for all) with the strongest effect in the theta band (4–8 Hz; $p = 0.007$, effect size $r = 0.49$). The neighboring age bins showed concordant though less significant differences (FNI > SC at week 34 for 4–13 Hz and FNI < SC at weeks 39–40 for 4–22 Hz; $p < 0.1$ for all). Validation analysis using active sleep epochs ($N = 301$) showed similar trajectories, with group differences appearing at the same time points (see Supplementary Fig. S4). However, these group differences did not pass conservative Benjamini–Hochberg FDR correction for multiple comparisons (4 frequencies \times 9 time points \times 2 sleep states = 72 tests). The O-information minima (Fig. 4B) was lower in the SC infants ($p < 0.1$) at 35 weeks in theta (4–8 Hz) and beta (13–22 Hz) bands, whereas at 38 weeks it became more negative for FNI (4–22 Hz; $p < 0.07$, $pFDR < 0.14$, effect size $0.32 < r < 0.46$). In turn, the optimal system size (Fig. 4C) at 35 weeks was larger in the SC group across the full bandwidth ($p < 0.1$), and most prominently in the alpha-beta band (8–22 Hz; $p < 0.016$, $pFDR = 0.036$ for both, effect size $r \geq 0.29$), but at 38 weeks it changed to opposite ($p < 0.034$, $pFDR < 0.054$, effect size $0.38 < r < 0.44$) except in the alpha band (8–13 Hz). Overall, these findings suggest that the synergistic scaffold in the brains of FNI infants develops more dynamically, yet steadily, before reaching term age. The cumulative effect of environmental enrichment intervention more likely causes the most prominent group difference just prior normal birth.

We then wanted to understand whether the environmental effects on the synergy development is reflected at the level of local maturation of neuronal

activity, as assessed by independent, machine learning-based estimates of the functional brain age (FBA⁴⁷) at each cortical parcel. There were significant, region-specific group differences (Wilcoxon rank-sum test) in the maturation of cortical neuronal activity (Fig. 4D). The group difference (SC > FNI) was first seen in the frontal regions (35 weeks; $p = 0.007$); it expanded to the whole cortex before term age (37 weeks; $p < 0.07$), followed by frontal and occipital group differences at around term age (38 weeks; $p < 0.05$). At term age, groups did not differ until week 42 when SC infants showed higher FBA in frontal and central regions ($p < 0.1$). FBA group differences did not reach the significance threshold ($pFDR < 0.05$) after Benjamini–Hochberg correction for multiple comparisons (4 regions \times 9 time points = 36 tests).

Taken together, the environmental enrichment appears to cause co-directional changes in the developmental trajectories of both the local neuronal activity (FBA) and the system-wide synergy (O-information), with the most prominent manifestation in the frontal regions (see also Fig. 2).

Discussion

Our results indicate that system-level organization of the infant brain is characterized by an early, region-specific shift from a functional structure dominated by redundant interactions to one dominated by synergistic interactions. Synergistic structure first emerges in the frontal lobe before spreading over other cortical areas in a specific spatiotemporal sequence, and this developmental trajectory can be modified by simple environmental modulations. The neurodevelopmental implication of redundancy/synergy balance was demonstrated by its significant correlation to later emerging neurocognitive functions.

The recent work in neuroscience on synergistic information in the brain builds on a historical body of work on self-organization in complex

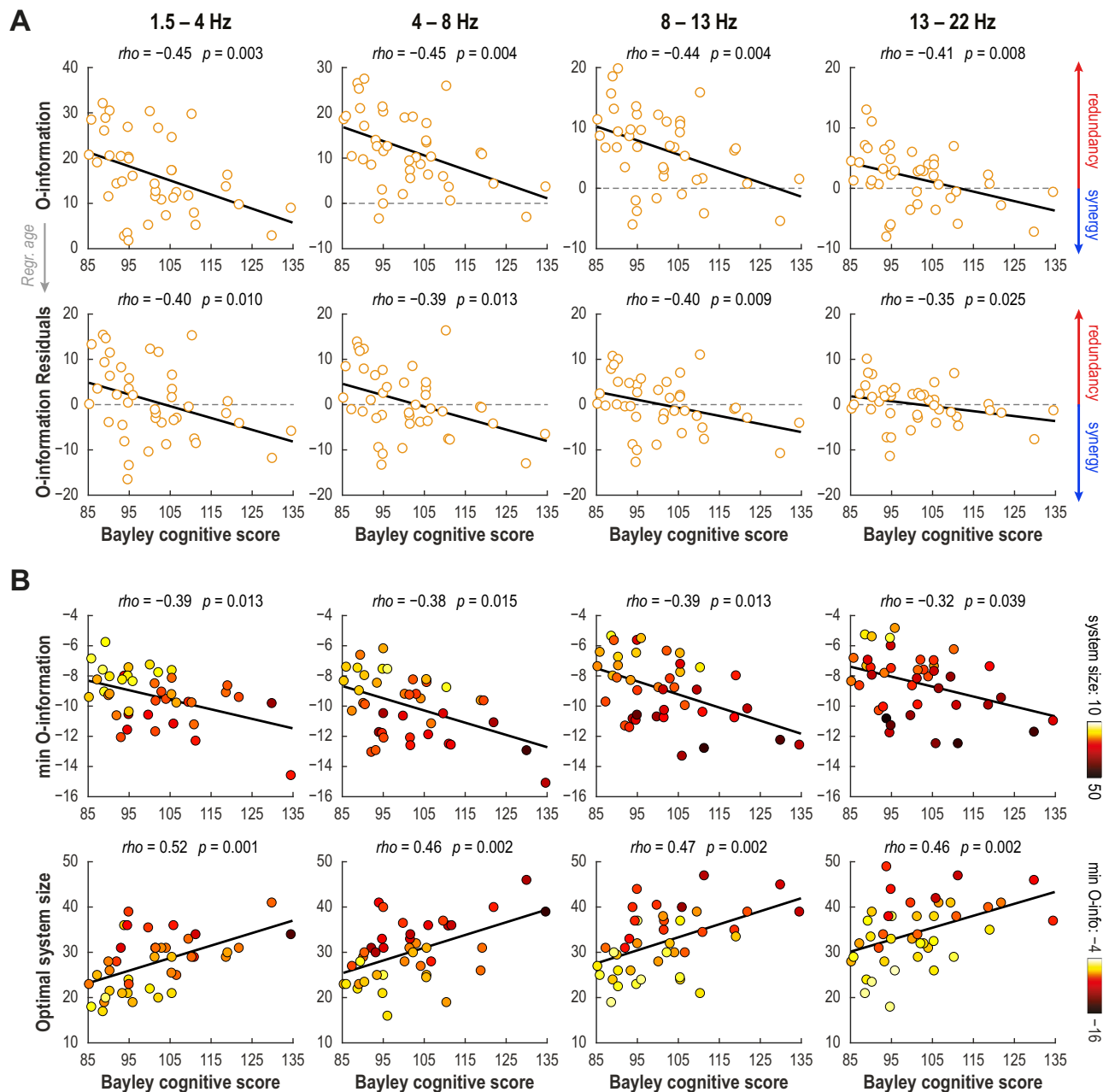


Fig. 3 | Synergy-dominated organization of the maturing brain associates with better neurodevelopment. **A** Correlation of the global O-information in the newborn brain and cognitive performance at 18 months of age. The upper panel shows the original values, whereas the lower one presents values after regressing age at EEG. **B** Both properties of the optimal sub-system: minimum O-information (upper row) and optimal sub-system size (lower row) correlate with future cognitive development. Colors of the dots cross-link two properties (minimum O-information to

optimal system size and vice versa). Overall, larger synergistic structures with higher level of synergy (more negative values of O-information minima) together were associated with better outcomes across all frequency bands. All EEG measures were taken from recordings near term age (38–42 weeks). The correlation analyses were done using Spearman test, and significance estimates are corrected post hoc for multiple comparisons.

systems. Kelso described “synergies” as forming “atomic” components of complex systems⁴⁸: basic units of function that emerge from the coordinated activity of multiple parts that nevertheless show a kind of “irreducible” behavior. The highly synergistic sub-systems identified by simulated annealing here might correspond to such “atomic” components of the larger synergistic scaffold. In this historical context, these kinds of synergies have typically been studied in the context of motor control^{49,50} and are distinct formally from the information-theoretic notions presented here, representing an alternative approach to the fundamental notion of an emergent whole that is greater than the sum of its constituent parts. Future work will focus on reconciling the diverse approaches to synergy that have been

explored in complex systems science and deepen our understanding of how complex “wholes” emerge from the interaction of many “parts.”

Prior work has established the presence of synergy in human fMRI data^{2,7,19}, and that the distribution of redundancies and synergies can change gradually during aging⁵, or more rapidly due to changes in the level of consciousness^{51,52}. Furthermore, neuroimaging studies have shown that the cortical areas with the richest synergistic information dynamics are associated with a variety of high-level cognitive processes and the expression of human-accelerated genes compared to non-human primates². Collectively, these results provide strong evidence that synergistic information is related to complex, higher-order cognition. The mechanistic relationship between

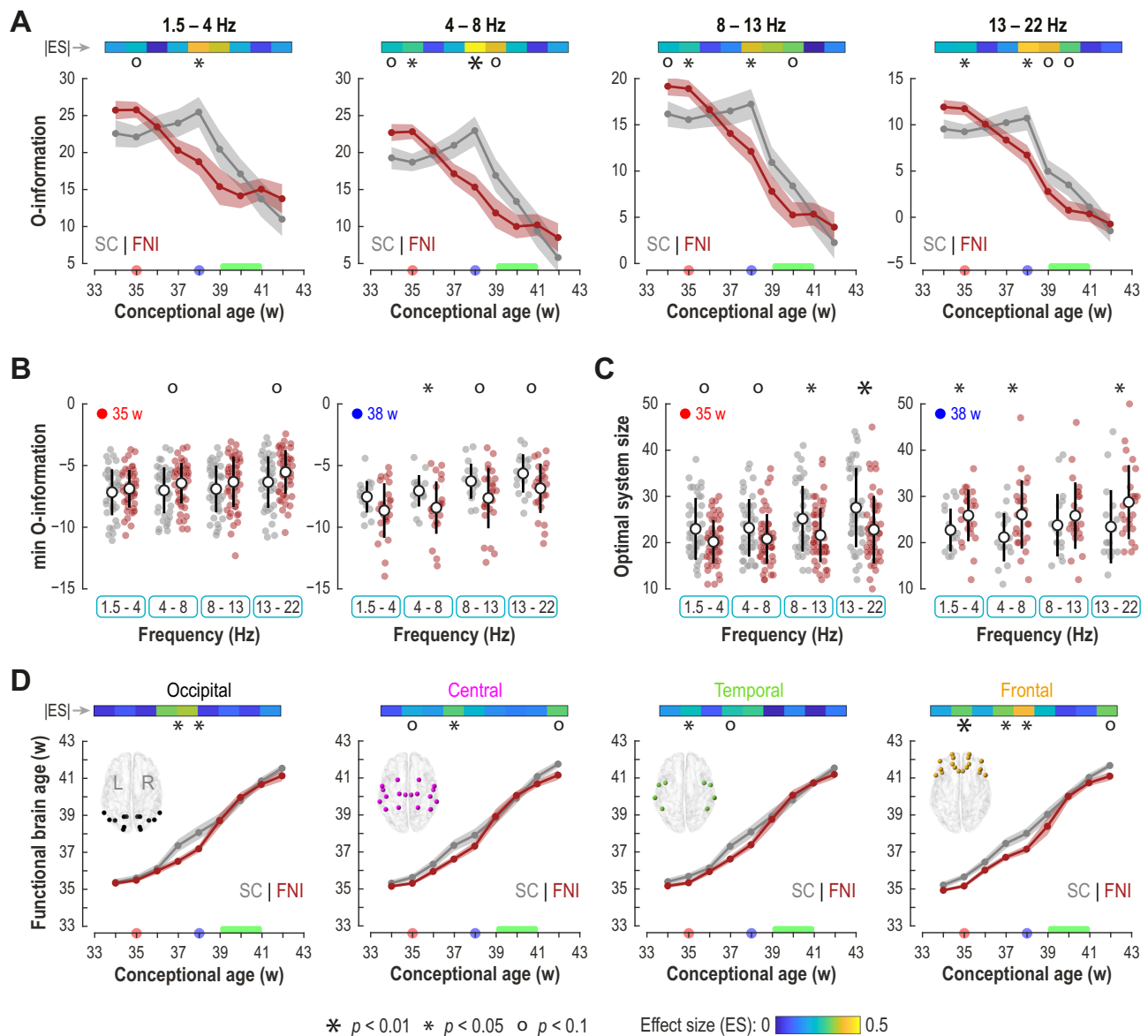


Fig. 4 | Environmental enrichment modulates global synergy and local maturity of neuronal activity. **A** Developmental trajectories in the global synergy (O-information) in the SC (gray) and FNI (dark red) groups at different frequency bands. Dots indicate group mean values computed at bi-weekly intervals and positioned at their midpoints, with shades depicting standard error of the mean (SEM); asterisks and circles indicate significant group differences (Wilcoxon rank-sum test, uncorrected). The bars on top show the absolute values of the effect size (ES) computed as rank-biserial correlation. The red and blue dots on the X-axis depict age points with the strongest consistent difference across all frequencies, which were selected for further analysis (in **B**) and **C**). The green bar depicts period corresponding to normal full-term birth. Note the differences in

developmental trajectories: FNI shows steady decrease, whereas SC is characterized by an initial “plateau” until a rapid decline occurs after about 38 weeks of age to reach the levels comparable to the FNI group. **B** Comparison of SC and FNI groups for O-information minima across different frequencies at the two time points marked in **A** (left, 35 weeks; right, 38 weeks). **C** Comparison of the optimal synergistic subsystem size for the same time points. In both **B** and **C**, individuals' values are shown with dots and the whiskers show mean (circle) and standard deviation (thick line), respectively. **D** Regional trajectories of local maturation in neuronal activity estimated by functional brain age (FBA) in the SC (gray) and FNI (dark red) groups. The FBA values (dots show infant group means; shade depicts SEM) in the graphs were computed as average of parcels in each cortical region.

synergy and cognition is still mysterious, however, as prior work has either been in *in silico* models (as in refs. 52,53) or in adults who have undergone extreme alterations to brain function, such as reversible anesthesia or disorders of consciousness following brain injury⁵¹. Our present work showed that synergy during sleep is significantly associated with later cognitive performance. This finding adds significantly to the prior literature, since it shows that meaningful neurocognitive correlates of synergy can be seen even in the sleeping brain at an ontogenetic stage prior to genuine cognitive performance. Moreover, the present findings suggest that synergy during pre-cognitive sleep may even predict the later neurodevelopmental potential of the brain; i.e., an ability to generate and maintain higher-order synergies

at a very early time in ontogenesis may support the developmental emergence of complex cognition later in life. This extends substantially the prior work that has shown acute correlations between synergy and level of consciousness^{51,52} or age⁵ in the short term, but has not shown a predictive relationship between information and cognition that extends over longer periods of time. This is consistent with work on artificial neural networks, where the synergy in individual “neurons” facilitates the capacity of the system to engage in multitasking and other integrative behaviors⁵³ (although analogies between artificial neural networks and human babies should be made with caution). Similarly, the finding that environmental enrichment early in life modulates the development of the synergistic structure suggests

that the presence (or absence) of synergy is at least partially mediated by complex multisensory experiences. Given this fact, as well as the aforementioned work linking a reduction in synergy to the loss of consciousness following anesthesia or traumatic brain injury⁵¹, our results also raise questions about the subjective nature of infant experience, and how it might change over the course of early development. The question of infant consciousness, or “what is it like to be an infant” is a philosophically complex one, made all the more puzzling because everyone was once an infant, but generally cannot recall any autobiographical details of the experience (if there is one)⁵⁴. Given the emerging literature suggesting that altered states of consciousness are associated with diverse changes to the information structure of brain activity, including changes to the complexity of brain activity writ large⁵⁵, we tentatively propose that the change from synchronized, redundancy-dominated dynamics to higher-order, synergy-dominated dynamics may be reflected in changes to the phenomenological quality of infant consciousness over development, although the exact nature of this relationship remains mysterious and is an area for further study.

Synergy may provide a fundamental mechanism that supports complex, higher brain functions characteristic of human behavior. Many higher neurobehavioural abilities in humans need efficient synergy to support communication within and between brain regions. The cellular underpinnings are characterized at all levels of neuronal communication, from synapses and cell types to different spatial scales in neuronal networks⁵⁶. In the context of the present findings, neuronal networks are likely the most fruitful level of explanation: At the microscale, comparisons to species that are phylogenetically more distant, such as rodents, indicate that the vast expansion of the human cortex comes with an evolutionary emergence of much denser interneuronal circuitry⁵⁷ to facilitate local information processing. At the mesoscale level, pyramidal neurons in the human cortex have evolved, exhibiting increased synaptic connectivity and many other unique input-output integration properties^{56,58}, which together improve information processing across cortico-cortical circuitries.

At the macroscale level, which is directly comparable to our present results, evolution of cortico-cortical network organization^{59,60} appears to be characterized by tuning the quality more than the quantity of connections. Despite larger brain size and higher anatomic variability in the human brain⁶¹, there appears to be a wider optimization of connection strengths (“weights”) that supports efficient macroscale information transfer^{62,63}. The early growth and organization of human neuronal networks is characterized by a prominent temporal overlap and prolongation of phases that would be temporally far more distinct in most other species^{56,61,64}. Such gradual network development provides an ideal framework for an activity- and experience-dependent development of macroscale synergy, i.e., a change in the functional network characteristics that needs rapid optimization of the connection strengths in the newly developed cortico-cortical networks. Moreover, this rationale would offer a mechanistic explanation for the finding that environmental enrichment may modulate the trajectories in synergy development: While the initial growth of neuronal connections is supported by the genetic code and endogenous neural activity^{15,18,26}, the following global organization including synergy in the neuronal networks is guided by neural activity that is sensitive to environmental and other acquired effects^{16,32,33,42}. The frontal lead in the emergence of functional synergy may be somewhat counterintuitive with respect to the general frontal delay in brain maturation^{65–68}. However, the existing literature is mainly based on structural measures whereas synergy in network activity characterizes informational signatures of macroscale interaction between neuronal ensembles: changes in the frontal region here reflect changes in the interactions between frontal neurons and potentially the rest of the brain. Recent studies have, indeed, highlighted the developmentally and functionally hierarchical brain organization, with clear gradients between sensory and association areas^{69–72}. The sensory areas develop to process information from inputs specific to the respective sensory modality that are only later communicated to higher order systems during postnatal life. In contrast, development of association areas, especially the frontal regions, is largely

characterized by optimizing information processing in the global cortico-cortical networks. Thus, emergence of macroscale synergy is inherently linked to early development of cortico-cortical circuitries in association areas, whereas corresponding synergy emerges much later in the sensory cortical areas.

The observed frequency dependence in the developing synergistic system aligns with a dynamic theory which combines prevailing general and infant-specific models of cortical activity. Due to the strong inverse relationship between spatial and oscillatory frequencies⁷³, the lower-frequency cortical activity arises from a larger spatial area, making the expected size of the optimal system smaller and more redundancy-dominated. Meanwhile, the hallmark of early cortical activity is an intermittent multifrequency bursting that gradually fades away after term age, while the continuous spontaneous EEG activity increases gradually and fully replaces the bursty patterns^{18,74,75}. These early EEG bursts are dominated by low-frequency activity⁷⁶ and are thought to provide temporal windows for interactions between spatially constrained and functionally more specific cortical areas across frequencies^{77,78}. As the infant develops closer to term age: i) the slowest waveforms are replaced by more rapid delta frequencies, ii) the higher frequency activity nested in the bursts will exhibit faster oscillations, and iii) the cortico-cortical interactions become more specific to reflect an increasing arealization. All these changes together converge in the link between lowering O-information in older infants and higher EEG frequencies.

The frontal lead in synergy development is also intriguingly compatible with our observation that the trajectories of synergy development are modulated by environmental enrichments (FNI group). Recent studies have established that human brain shows particularly protracted developmental time spans across many level⁷⁹: The anatomical studies from the months around birth indicate several months-long coexistence of overlapping macroscale connectivity⁸⁰, whereas many synaptic characteristics^{65,81,82} or molecular expression profiles^{81,83} show a strong neoteny persisting until late childhood. Such a protracted and gradual development renders the system modifiable or able to learn through the well-established activity-dependent process; however, it also makes the developing brain subject to environmental effects, such as perturbations by medical adversities. Here, we postulate that the trajectory of synergy development in the FNI group represents the natural course as it would happen *in utero*. Conversely, the biphasic trajectory in the SC group reflects an initial slowing down of synergy development by the prematurity-related medical adversities³², followed by a rapid catch-up near-term age. Intriguingly, a transient developmental FNI effect was also seen in the independent maturation measure (FBA) of the local neuronal activity. Our current FBA results are in line with the literature suggesting that premature birth may lead to an apparent accelerated maturation of newborn brain activity^{84,85} and structural brain development in later life^{86,87}. Moreover, other works on the newborns have shown that prematurity also leads to persistent changes in large-scale functional cortico-cortical networks^{31,74,88–90}, which may be substantially reduced by environmental enrichment²². It is important in this context, however, that early neurodevelopmental cascades are too complex to assume a direct link from faster changing single measures to better neurodevelopmental outcomes. Instead, the biologically optimal development is best characterized by charting the typical developmental trajectory of each measure independently, and thereby, any deviance from this normal trajectory implies an altered development. The systems-level developmental cascades of these neuronal mechanisms call for future studies with cross-species translatable measures, such as the O-information used in our present work.

Our present results and prior studies together suggest that environmental effects may substantially modulate the early organization of functional brain networks. Both the early development of cortico-cortical network activity and the emergence of brain synergy build on co-stabilization of the long-range axonal conduction via myelination^{91,92} and the local synaptic transmission⁸². Experimental studies have indicated these factors in recovery from brain injury^{93,94}, learning and development⁹², as well as in the brain response to early environmental enrichment interventions^{95,96}. While it appears widely accepted that very early

environmental modulation, or nurturing, can improve later neurodevelopment⁹⁷, understanding the underlying neuronal mechanisms needs substantially more systematic and translational work, preferably in phylogenetically aligned animal models.

Our study has some limitations. The EEG dataset comes from a clinical trial that was powered to show trial-related effects, and here we used all available EEG data without an a priori sample size calculation. However, the many significant and biologically sound findings in our exploratory study support a notion that our sample size was adequate for seeing many key effects. We cannot exclude the possibility that further findings could be found with even larger samples, which, however, are very rare in the human neonatal research worldwide. The data analyses included 5 minutes of artifact-free high-density state-specific infant EEG, and more data would always be desirable. Obtaining more quality EEG signal from all cohort subjects is very challenging in the human infants, and therefore most research to date is performed with much less data. However, prior studies have shown that this data length is already sufficient to provide reliable and stable estimates from the cortical network activities^{22,31}. Moreover, we also validated many key findings by using EEG epochs from two different sleep states (active sleep and quiet sleep), providing a total of 10 min EEG data from two different vigilance states. Another limitation is the comparatively small number of cortical regions included in our analysis, and the lack of good subcortical coverage. Consequently, these results show only a partial picture of the global organization of higher-order information in the developing brain. The fact that we used data from sleeping infants is a significant departure from previous work on synergy and brains^{2,51,52}, which typically compares normal, wakeful rest against altered states such as anesthesia, brain injury, or aging, or over the course of aging^{5,98}. This makes direct comparison with our results non-trivial, although increasing the diversity of data types and experimental frameworks will help us better understand the role that synergistic information plays in many facets of neural activity.

There are also limitations inherent in the use of Gaussian estimators of the O-information, as applied to EEG data, which is typically non-normally distributed and may not be consistently stationary. Gaussian estimators were chosen for several reasons: the first is consistency with prior studies of synergy in brain data (e.g., refs. 2,19,51). The second is to avoid discretizing continuous data, which would result in a massive loss of information, as well as introducing bias/variance trade-offs associated with discrete entropy estimators⁹⁹. The third was because the simulated annealing optimization requires a large number of very rapid estimates of the O-information, which rules out non-parametric estimators based on K-nearest neighbors methods such as the Kozachenk-Leonenko entropy estimator^{100,101} or the Kraskov mutual information estimator¹⁰². Future developments in non-parametric entropy and information estimators will improve our capacity to detect non-linear, higher-order structures in electrophysiological brain data.

Finally, it is worth reflecting on the implications of these and other results that use higher-order information theory to explore brain activity. The standard approaches based on single regions, or pairwise region-to-region interactions (commonly used in network models) capture only a very small subset of all possible dependencies that co-exist and interact in the brain. Our present approach with a very dense scalp EEG recording allowed assessment of approximately 3 thousand possible directed interactions, which is at the physical limits of spatial resolution available in studying neuronal activity in human infants³¹. If we consider the possibility of higher-order synergies up to the 5th order, then the total number of possible dependencies expands to approximately 7 million interactions. The network then represents only 0.0005% of the possible structure of the system (stopping at 5th order interactions; we can, of course, go higher). This “shadow structure”^{7,19} represents a vast space of largely unexplored structured brain activity. Our results here show that this space contains patterns of multivariate information that are associated with, and possibly promote, specific aspects of human development, cognition, and parent-child interactions. Future work exploring this higher-order space may yet yield further, fruitful insights into the nature of brain, mind, and behavior.

Methods

Subjects and background information

We analyzed EEG dataset from $N = 136$ preterm infants (born at 31 ± 2.4 weeks; mean \pm std) that was collected during the Family Nurture Intervention (FNI) randomized controlled trial (#NCT01439269 in ClinicalTrials.gov) in Morgan Stanley Children’s Hospital of New York at the Columbia University Medical Center⁴³. The general dataset consisted of two subgroups: standard care infants (SC; $N = 62$, born 30.9 ± 2.5 weeks), and those who additionally underwent intervention aimed to facilitate mother-infant emotional connection (FNI; $N = 74$, born 31.2 ± 2.3 weeks). Subgroups showed no difference in the age of birth ($p = 0.8$, Wilcoxon ranksum test). Review Board at Columbia University Medical Center (NY, USA) approved study and recruitment procedures. Written consents were obtained from mothers before the start of the intervention. The detailed description of the FNI protocol was published previously^{43,103,104}. In brief, intervention for FNI infants started in average one week after delivery and the frequency of the sessions was 3–4 times per week during the period of hospitalization under supervision of nurture specialist. Each session lasted about one hour, during which mothers had skin-to-skin contact with their babies, exchanged scent cloths, touched them, were making eye contact as much as possible, and spoke about their feelings. EEG recordings from FNI subjects were done not during the contact sessions, but at separately designated times. Importantly, FNI activities were provided in addition to the standard care protocol, which was applied to all subjects in both groups. In turn, SC was mainly focused on the maintenance of infant temperature in isolette, oxygen and nutrition support, prevention and treatment of infections, and parent education about temperature checking, breast feeding, bathing, diaper change, cardiopulmonary resuscitation⁴³.

EEG recordings

EEG data was collected longitudinally between weeks 33 and 45 of conceptual age during daytime sleep using 128-channel system Electrical Geodesics system. (EGI, Inc., Eugene, Oregon). EEG electrodes were sponges soaked with physiological saline. After consultation with the manufacturer, we also covered the electrode net with plastic wrap to avoid the evaporation of the saline and to archive good electrode-scalp contact and then also with special elastic material (“Surgilast”). Each session lasted for about one hour and covered at least one full sleep cycle comprising periods of active and quiet sleep¹⁰⁵. Four facial electrodes were excluded from further analysis leading to final 124 EEG channels per infant. During the recordings the impedance of EEG electrodes was kept below 50 kilohms. Original recordings were done using vertex electrode as a reference, with a sampling rate $F_s = 1$ kHz, and using band-pass filter 0.1–400 Hz. After the recording, all data were re-referenced to average montage.

EEG pre-processing

First, we identified periods of stable quiet sleep (precursor of non-rapid eye movement sleep) from the whole recording using conventional criteria¹⁰⁶. We opted to use quiet sleep in all the analyses because EEG during this state is phenomenologically more discriminative: it has discontinuous structure comprising bursts of activity and in-between silent intervals^{74,75}. Moreover, quiet sleep EEG epochs are technically more stable: they contain less electromyographic and electrooculographic artifacts as well as noise associated with movement. However, for cross-validation of some key analyses we also classified the epochs of active sleep (precursor of rapid eye movement sleep) which is characterized by more continuous EEG signals. Next, all selected epochs were visually reviewed to identify prominent artifacts such as bad or absence of skin-electrode contact, presence of electromyogram, and cable movement. Further we applied independent component analysis (ICA) to check for the presence of electrocardiographic artifact in every recording and removed it where it was detected. ICA was also used to check and clean rare artifacts caused by interference of other medical devices in neonatal intensive care unit. For the analysis we selected 5 minutes of artifact-free EEG (separately during quiet and active sleep) by combining ten equidistant 30-second-long windows across the whole available recording of each

specific state. That was done to overcome variability in available EEG lengths across different subjects and to obtain representative epochs that characterize the whole period of each sleep state. Channels that were bad across entire recording session were removed from further analysis (9.4 ± 4.5 per subject; mean \pm std). Our recent study showed that, for infant recordings with high-density EEG nets, excluding this number of electrodes does not significantly impact the reconstruction quality of the cortical parcel signals¹⁰⁷. The final dataset included $N = 289$ EEG recordings (from $N = 134$ subjects) during quiet sleep and $N = 301$ EEG recordings (from $N = 135$ subjects) during active sleep, which satisfied both quality and length requirements: $N = 30$ infants with one recording, $N = 51$ with two recordings, $N = 51$ with three recordings, and $N = 1$ with four recordings. More detailed information on the sample sizes and the times of EEG recordings can be found in Supplementary Fig. S1. These recordings then were band-pass filtered within frequency range 0.4–40 Hz and down sampled to $F_s = 100$ Hz.

Computation of cortical signals

Scalp-level EEG signals were reconstructed into cortical signals using three-shell general infant head model^{9,108}. The model included scalp, skull, and intracranial volume boundaries approximated with 2562 vertices per compartment and having conductivities 0.43 S/m, 0.2 S/m, and 1.79 S/m respectively^{109–111}. Source space was represented by 8014 dipoles with fixed orientation and orthogonal to the cortical surface. To avoid the influence of developmental changes and inter-individual variability in cortical geometry on our results, we opted to project all EEG data onto cortical template of full-term infant which is about in the middle of the studied age range. Forward operator was computed using symmetric boundary element method¹¹². Whereas, inverse operator was computed with dynamic statistical parametric mapping approach¹¹³ as it is implemented in Brainstorm¹¹⁴. All sources were further collapsed into 58 cortical parcels using infant parcellation scheme³¹. Next, based on their overlap with brain anatomical regions, all parcels were categorized into frontal ($N = 18$), central ($N = 18$), occipital ($N = 14$), and temporal ($N = 8$). Cortical signals were computed as the weighted mean of all underlying source signals within the host parcels. To compute functional brain age (see section below), we used broad-band (0.4–40 Hz) cortical signals. However, to study developmental trajectories of O-information measures, we further filtered cortical signals into four frequency bands of interest: delta (1.5–4 Hz), theta (4–8 Hz), alpha (8–13 Hz), and beta (13–22 Hz). All band-pass filtering in this work was implemented by using combinations of high-pass and low-pass Butterworth filters with the corresponding cut-offs. Filters were applied offline and in forward-backward directions to avoid distortions of phases caused by infinite impulse response filters. The attenuation in the stopband in one direction was at least 15 dB.

Association with neurodevelopment

We correlated (Spearman test) O-information measures computed for infant brain around term age (38–40 weeks) to Bayley scales (BSID-III) cognitive scores²³ assessed at 1.5 years of age. Bayley scales is the most widely used, standardized neuropsychological assessment, and it is often taken as the norm in clinical research²⁴. It consists of a larger test battery measuring different subdomains of neurological and cognitive performance (cognition, motor, language, social). In the present work, we studied the cognitive domain only, because it reflects brain functions that are most directly linked to global interactions in the cortical activity, such as the O-information. Specifically, the assessment of the cognitive score includes tasks that test attention to familiar and unfamiliar objects, visual tracking, memory, problem-solving, and sensory processing abilities. Following the recommended criteria¹¹⁵, we excluded subjects with moderate and severe neurodevelopmental delay (cognitive scores < 85) from this analysis. Initially, there were $N = 50$ subjects with both EEG at this age and outcomes, but $N = 9$ of them were excluded. There was no significant difference in O-information between included into correlation analysis and excluded subjects ($p > 0.11$ for all frequencies; Wilcoxon rank-sum test). For subjects with two

recordings ($N = 3$) falling into the age range of interest, we used average of their O-information indices. Consequently, $N = 41$ infants were included in the correlation analysis. To exclude the impact of the developmental changes, we also computed same correlations after regressing conceptional ages from O-information measures (see Fig. 3A). Finally, we used Benjamini–Hochberg procedure to control for multiple comparisons (across four frequency bands).

Higher-order information analysis

To assess the emergence of higher-order, coordinated brain activity involving multiple regions, we used measures from information theory¹¹⁶. When considering how groups of three or more brain regions share information, there is a distinction to be made between different kinds of higher-order interaction¹¹⁷. Some information is stored *redundantly*: it is duplicated over individual brain regions and so could be learned by observing Region 1 alone or Region 2 alone or Regions 3 alone, and so on. The alternative is information that is stored *synergistically*, in the joint-state of two or more regions. This is information that can only be learned by knowing the state of Region 1 and Region 2 and Region 3, and so on. For a more detailed discussion of redundancy, synergy, and logical implicature, see refs. 118,119. Synergistic information requires a high degree of coordination between multiple regions, forming an integrated “whole” that is “greater than the sum of its parts”¹⁹.

To explore the distribution and redundancies across the developing neonatal cortex, we used a recently proposed, information-theoretic measure: the O-information²⁰. A heuristic measure, for a multivariate system \mathbf{X} , the O-information of that system, $\Omega(\mathbf{X})$ reflects whether the information structure of the system is redundancy-dominated (in which case, $\Omega(\mathbf{X}) > 0$) or synergy-dominated (in which case, $\Omega(\mathbf{X}) < 0$).

For a more detailed, mathematical analysis of the O-information, see the original proposal by Rosas et al.²⁰. Briefly, the O-information begins with a simpler measure that generalizes the bivariate Shannon mutual information to arbitrarily large systems. Originally introduced by Watanabe as the total correlation¹²⁰ and then independently re-derived by Tononi, Sporns, and Edelman as the integration¹²¹, the total correlation is defined by:

$$TC(\mathbf{X}) = \left(\sum_{i=1}^N H(X_i) \right) - H(\mathbf{X}) \quad (1)$$

where $N = |\mathbf{X}|$, and $H()$ is the Shannon entropy function. The total correlation can be thought of as a measure of redundancy: $TC(\mathbf{X})$ is maximal when every X_i is a copy of every other variable. Varley et al. showed that the O-information can be written in terms of sums and differences of total correlations¹⁹:

$$\Omega(\mathbf{X}) = (2 - N)TC(\mathbf{X}) + \sum_{i=1}^N TC(\mathbf{X}^{-i}). \quad (2)$$

Where \mathbf{X}^{-i} indicates the joint state of every element of \mathbf{X} excluding X_i . For instance, if $\mathbf{X} = \{X_1, X_2, X_3, X_4\}$, then $\mathbf{X}^{-2} = \{X_1, X_3, X_4\}$. We can intuitively understand $\Omega(\mathbf{X})$ as quantifying the difference between the integration of the “whole” and the integration the “parts.” The left-hand term, $(2 - N)TC(\mathbf{X})$ is the integration of the whole \mathbf{X} , duplicated $(2 - N)$ times (and is therefore a large, negative number, as N is always greater than two in higher-order interactions). The right-hand side, $\sum_{i=1}^N TC(\mathbf{X}^{-i})$ can be understood as adding back in the integration of every lower-order ensemble that excludes one element each time. If $(2 - N)TC(\mathbf{X}) > \sum_{i=1}^N TC(\mathbf{X}^{-i})$, then there is integration in the whole that is not accounted for by the sum of the lower order parts. This is why $\Omega(\mathbf{X}) < 0$ is taken as a heuristic indicator of synergy.

Given the continuous nature of electrophysiological signals, we used Gaussian estimators of the differential total correlation¹²¹:

$$TC(\mathbf{X}) = \frac{-\ln |\Sigma_{\mathbf{X}}|}{2} \quad (3)$$

where $|\Sigma_X|$ is the determinant of the covariance matrix of \mathbf{X} . For every recording, we computed global O-information and global total correlation for the entire brain.

Simulated annealing to extract synergistic subsystems

Following Varley et al.¹⁹, we used a variant of the simulated annealing algorithm¹²² to extract maximally synergistic ensembles of brain regions. Briefly, given a fixed ensemble k brain regions, the simulated annealing algorithm begins with a random set of k brain regions, and then swaps regions in and out to minimize the objective function (in this case, the O-information). Prior work in adult, human neuroimaging data has shown that optimally synergistic O-information has a non-monotonic relationship with k ¹⁹. Consequently, we ran the optimization for every integer value of k in the range 3–57.

Since O-information is a measure of redundancy/synergy bias, for a given optimal ensemble of size k , it cannot be assumed that the k elements are not “compromised” by the presence of redundancy. For example, one could imagine that the annealing algorithm returns a set \mathbf{X}^* of five regions, where three regions are highly synergistic amongst themselves, while the other two regions are independent, or perhaps weakly redundant. Claiming that the $\Omega(\mathbf{X}^*)$ represents a synergistic dependency between all five elements would be spurious. Following¹⁹, for every optimal bag \mathbf{X}^* , we used a filtering algorithm: if the removal of any single element from \mathbf{X}^* decreases the O-information, then we say that the set \mathbf{X}^* is not “irreducibly synergistic” and removed it from our analysis.

Developmental trajectories

We produced developmental trajectories for infants’ subgroups (FNI and SC) by computing mean values within 2-weeks-wide sliding windows with 50% overlap (Fig. 4A). These settings were selected as a compromise between temporal resolution and the sample sizes. Further, clinical groups were compared in each age bin using Wilcoxon rank-sum test. For the age bins which showed consistent group differences in O-information across all frequency bands (35 and 38 weeks), we also compared minima of O-information and optimal subsystem size. The same approach was used also for functional brain age courses (Fig. 4D). Effect size of the group differences was estimated using rank-biserial correlation (r).

Computation of functional brain age

Functional brain age (FBA) was estimated based on the combination of several features extracted from the 5-minute-long cortical signals. A total of $N=43$ features were extracted from the signals. These features were designed to summarize the amplitude, frequency, and information content of the brain signals; cross-channel/parcel measurements were removed as regionally specific evaluation of FBA was the aim of analysis⁴⁷. Features were estimated from each cortical signal and then averaged across all parcels within an anatomical region (four regions were used: frontal, central, temporal, and occipital). The 43 features per region were then combined using support vector regression to calculate FBA estimate¹²³. The combination was trained within a 10-fold cross validation, where approximately 90% of cortical signals were included in a training set, and 10% of cortical signals were left out for testing. This process that was repeated 10 times until all data had been tested. Due to the presence of multiple EEG recordings and twins in the dataset, cross-validation selections were based on mother’s ID number. Within each training fold, feature selection was applied using a hybrid filter-wrapper approach to reduce the dimensionality of the input feature vector¹²⁴. As a first stage, only features with a significant correlation with age (corrected for multiple comparisons; Benjamini–Hochberg procedure) were selected (filter stage). The residual feature set was applied to a backwards feature selection as a second stage, with a stopping criterion based on the Akaike Information Criterion evaluated on an internal 4-fold cross-validation (wrapper stage). The SVR was trained using the Matlab function `fitrsvm.m` with a medium Gaussian kernel (Kernel Scale = 9.8, box constraint = $\text{IQR}/1.349$, $\epsilon = \text{IQR}/13.49$ and IQR is the interquartile range

the input ages). The process of training the FBA was for each anatomical region resulting in 4 FBAs per infant EEG recording.

Statistics and reproducibility

In this work, we used statistical tests as implemented in MATLAB 2021a. Covariance matrices were computed from z-scored cortical signals. Correlations were assessed using Spearman’s method. Group comparisons were performed using the Wilcoxon rank-sum test. To control for multiple comparisons, we applied the Benjamini–Hochberg correction. To determine whether nodes from specific anatomical regions were overrepresented in group-level synergistic scaffolds beyond chance, we used binomial statistics. More details on statistical analyses can be found in the corresponding sections. See sections “Code availability” and “Data availability” for reproducibility.

Reporting summary

Further information on research design is available in the Nature Portfolio Reporting Summary linked to this article.

Data availability

The EEG data analyzed in this work are available through a data sharing agreement with Columbia University Medical Center (NY, USA). Data for reproducing figures can be found in Supplementary Data.

Code availability

The MATLAB code for computing O-information is provided in Supplementary Code 1, and the code for visualizing synergistic scaffolds is provided in Supplementary Code 2. The MATLAB code for computing FBA is available on GitHub: <https://github.com/nstevensonUH/Neonatal-EEG-Analysis>.

Received: 22 July 2024; Accepted: 11 April 2025;

Published online: 13 May 2025

References

1. Gutknecht, A. J., Wibral, M. & Makkeh, A. Bits and pieces: understanding information decomposition from part-whole relationships and formal logic. *Proc. Math. Phys. Eng. Sci.* **477**, 20210110 (2021).
2. Luppi, A. I. et al. A synergistic core for human brain evolution and cognition. *Nat. Neurosci.* **25**, 771–782 (2022).
3. Luppi, A. I., Rosas, F. E., Mediano, P. A. M., Menon, D. K. & Stamatakis, E. A. Information decomposition and the informational architecture of the brain. *Trends Cogn. Sci.* **28**, 352–368 (2024).
4. Varley, T. F. Information theory for complex systems scientists. *arXiv* <https://doi.org/10.48550/arXiv.2304.12482> (2023).
5. Gatica, M. et al. High-order interdependencies in the aging brain. *Brain Connect.* **11**, 734–744 (2021).
6. Newman, E. L., Varley, T. F., Parakkattu, V. K., Sherrill, S. P. & Beggs, J. M. Revealing the dynamics of neural information processing with multivariate information decomposition. *Entropy* **24**, 930 (2022).
7. Varley, T. F., Pope, M., Maria, G., Faskowitz, J. & Sporns, O. Partial entropy decomposition reveals higher-order information structures in human brain activity. *Proc. Natl Acad. Sci. USA* **120**, e2300888120 (2023).
8. Varley, T. F., Sporns, O., Schaffelhofer, S., Scherberger, H. & Dann, B. Information-processing dynamics in neural networks of macaque cerebral cortex reflect cognitive state and behavior. *Proc. Natl Acad. Sci. USA* **120**, e2207677120 (2023).
9. Tokariev, A., Videman, M., Palva, J. M. & Vanhatalo, S. Functional brain connectivity develops rapidly around term age and changes between vigilance states in the human newborn. *Cereb. Cortex* **26**, 4540–4550 (2016).

10. Batalle, D. et al. Early development of structural networks and the impact of prematurity on brain connectivity. *Neuroimage* **149**, 379–392 (2017).
11. Keunen, K., Counsell, S. J. & Benders, M. J. The emergence of functional architecture during early brain development. *Neuroimage* **160**, 2–14 (2017).
12. Turk, E. et al. Functional connectome of the fetal brain. *J. Neurosci.* **39**, 9716–9724 (2019).
13. Kostovic, I., Radoš, M., Kostovic-Srzentic, M. & Krsnik, Z. Fundamentals of the development of connectivity in the human fetal brain in late gestation: from 24 weeks gestational age to term. *J. Neuropathol. Exp. Neurol.* **80**, 393–414 (2021).
14. Karolis, V. R. et al. Maturation networks of human fetal brain activity reveal emerging connectivity patterns prior to ex-utero exposure. *Commun. Biol.* **6**, 661 (2023).
15. Luhmann, H. J. et al. Spontaneous neuronal activity in developing neocortical networks: from single cells to large-scale interactions. *Front. Neural Circuits* **10**, 40 (2016).
16. Molnár, Z., Luhmann, H. J. & Kanold, P. O. Transient cortical circuits match spontaneous and sensory-driven activity during development. *Science* **370**, eabb2153 (2020).
17. Martini, F. J., Guillaumon-Vivancos, T., Moreno-Juan, V., Valdeolmillos, M. & López-Bendito, G. Spontaneous activity in developing thalamic and cortical sensory networks. *Neuron* **109**, 2519–2534 (2021).
18. Luhmann, H. J., Kanold, P. O., Molnár, Z. & Vanhatalo, S. Early brain activity: translations between bedside and laboratory. *Prog. Neurobiol.* **213**, 102268 (2022).
19. Varley, T. F., Pope, M., Faskowitz, J. & Sporns, O. Multivariate information theory uncovers synergistic subsystems of the human cerebral cortex. *Commun. Biol.* **6**, 451 (2023).
20. Rosas, F. E., Mediano, P. A. M., Gastpar, M. & Jensen, H. J. Quantifying high-order interdependencies via multivariate extensions of the mutual information. *Phys. Rev. E* **100**, 032305 (2019).
21. Myers, M. M. et al. Family Nurture Intervention in preterm infants alters frontal cortical functional connectivity assessed by EEG coherence. *Acta Paediatr.* **104**, 670–677 (2015).
22. Yrjölä, P. et al. Facilitating early parent-infant emotional connection improves cortical networks in preterm infants. *Sci. Transl. Med.* **14**, eabq4786 (2022).
23. Bayley, N. *Bayley Scales of Infant and Toddler Development* 3rd. edn (Harcourt Assessment, 2006).
24. Welch, M. G. et al. Family nurture intervention in the neonatal intensive care unit improves social-relatedness, attention, and neurodevelopment of preterm infants at 18 months in a randomized controlled trial. *J. Child Psychol. Psychiatry* **56**, 1202–1211 (2015).
25. Alex, A. M. et al. Genetic influences on the developing young brain and risk for neuropsychiatric disorders. *Biol. Psychiatry* **93**, 905–920 (2023).
26. Zhou, Y., Song, H. & Ming, G.-I. Genetics of human brain development. *Nat. Rev. Genet.* **25**, 26–45 (2024).
27. Sale, A. A systematic look at environmental modulation and its impact in brain development. *Trends Neurosci.* **41**, 4–17 (2018).
28. Miguel, P. M., Pereira, L. O., Silveira, P. P. & Meaney, M. J. Early environmental influences on the development of children's brain structure and function. *Dev. Med. Child Neurol.* **61**, 1127–1133 (2019).
29. Nolvi, S., Merz, E. C., Kataja, E.-L. & Parsons, C. E. Prenatal stress and the developing brain: postnatal environments promoting resilience. *Biol. Psychiatry* **93**, 942–952 (2023).
30. Rubinstein, M. R., Burqueño, A. L., Quiroga, S., Wald, M. R. & Genaro, A. M. Current understanding of the roles of gut-brain axis in the cognitive deficits caused by perinatal stress exposure. *Cells* **12**, 1735 (2023).
31. Tokariev, A. et al. Large-scale brain modes reorganize between infant sleep states and carry prognostic information for preterms. *Nat. Commun.* **10**, 2619 (2019).
32. Inder, T. E., Volpe, J. J. & Anderson, P. J. Defining the neurologic consequences of preterm birth. *N. Engl. J. Med.* **389**, 441–453 (2023).
33. Russ, J. B. & Ostrem, B. E. L. Acquired brain injuries across the perinatal spectrum: pathophysiology and emerging therapies. *Pediatr. Neurol.* **148**, 206–214 (2023).
34. Syvälahti, T. et al. Networks of cortical activity show graded responses to perinatal asphyxia. *Pediatr. Res.* **96**, 132–140 (2024).
35. Georgieff, M. K., Ramel, S. E. & Cusick, S. E. Nutritional influences on brain development. *Acta Paediatr.* **107**, 1310–1321 (2018).
36. Fitzgerald, E., Hor, K. & Drake, A. J. Maternal influences on fetal brain development: the role of nutrition, infection and stress, and the potential for intergenerational consequences. *Early Hum. Dev.* **150**, 105190 (2020).
37. Tokariev, A. et al. Impact of in utero exposure to antiepileptic drugs on neonatal brain function. *Cereb. Cortex* **32**, 2385–2397 (2022).
38. Han, Y. et al. The role of enriched environment in neural development and repair. *Front. Cell Neurosci.* **16**, 890666 (2022).
39. Lordier, L. et al. Music in premature infants enhances high-level cognitive brain networks. *Proc. Natl Acad. Sci. USA* **116**, 12103–12108 (2019).
40. Haslbeck, F. B. et al. Creative music therapy to promote brain function and brain structure in preterm infants: a randomized controlled pilot study. *NeuroImage Clin.* **25**, 102171 (2020).
41. Charpak, N. et al. Kangaroo mother care had a protective effect on the volume of brain structures in young adults born preterm. *Acta Paediatr.* **111**, 1004–1014 (2022).
42. Belrán, M. I., Dudink, J., de Jong, T. M., Benders, M. J. N. L. & van den Hoogen, A. Sensory-based interventions in the nicu: systematic review of effects on preterm brain development. *Pediatr. Res.* **92**, 47–60 (2022).
43. Welch, M. G. et al. Family nurture intervention (fni): methods and treatment protocol of a randomized controlled trial in the nicu. *BMC Pediatr.* **12**, 14 (2012).
44. Moore, E. R., Bergman, N., Anderson, G. C. & Medley, N. Early skin-to-skin contact for mothers and their healthy newborn infants. *Cochrane Database Syst. Rev.* **11**, Cd003519 (2016).
45. Welch, M. G. & Myers, M. M. Advances in family-based interventions in the neonatal icu. *Curr. Opin. Pediatr.* **28**, 163–169 (2016).
46. Welch, M. G. et al. Family nurture intervention increases term age forebrain eeg activity: a multicenter replication trial. *Clin. Neurophysiol.* **138**, 52–60 (2022).
47. Stevenson, N. J. et al. Automated cot-side tracking of functional brain age in preterm infants. *Ann. Clin. Transl. Neurol.* **7**, 891–902 (2020).
48. Kelso, J. A. S. Synergies: atoms of brain and behavior. in *Progress in Motor Control: A Multidisciplinary Perspective* (ed. Sternad, D.) 83–91 (Springer, 2009).
49. Sternad, D. (ed.) *Progress in Motor Control: A Multidisciplinary Perspective, Vol. 629 of Advances in Experimental Medicine and Biology* (Springer, 2009).
50. Kelso, J. A. S. On the coordination dynamics of (animate) moving bodies. *J. Phys. Complex.* **3**, 031001 (2022).
51. Luppi, A. I. et al. A synergistic workspace for human consciousness revealed by integrated information decomposition. *eLife* **12**, RP88173 (2024).
52. Luppi, A. I. et al. Reduced emergent character of neural dynamics in patients with a disrupted connectome. *NeuroImage* **269**, 119926 (2023).
53. Proca, A. M. et al. Synergistic information supports modality integration and flexible learning in neural networks solving multiple tasks. *arXiv* <https://doi.org/10.48550/arXiv.2210.02996> (2022).

54. Bayne, T., Frohlich, J., Cusack, R., Moser, J. & Naci, L. Consciousness in the cradle: on the emergence of infant experience. *Trends Cogn. Sci.* **27**, 1135–1149 (2023).
55. Sarasso, S. et al. Consciousness and complexity during unresponsiveness induced by propofol, xenon, and ketamine. *Curr. Biol.* **25**, 3099–3105 (2015).
56. Vanderhaeghen, P. & Polleux, F. Developmental mechanisms underlying the evolution of human cortical circuits. *Nat. Rev. Neurosci.* **24**, 213–232 (2023).
57. Loomba, S. et al. Connectomic comparison of mouse and human cortex. *Science* **377**, eabo0924 (2022).
58. Schmidt, E. R. E. et al. A human-specific modifier of cortical connectivity and circuit function. *Nature* **599**, 640–644 (2021).
59. Knoblauch, K., Ercsey-Ravasz, M., Kennedy, H. & Toroczkai, Z. *The Brain in Space* 45–74 (Springer, 2016).
60. Puxeddu, M. G. et al. Relation of connectome topology to brain volume across 103 mammalian species. *PLoS Biol.* **22**, e3002489 (2024).
61. Van Essen, D. C. et al. Cerebral cortical folding, parcellation, and connectivity in humans, nonhuman primates, and mice. *Proc. Natl Acad. Sci. USA* **116**, 26173–26180 (2019).
62. Markov, N. T. et al. A weighted and directed interareal connectivity matrix for macaque cerebral cortex. *Cereb. Cortex* **24**, 17–36 (2014).
63. Oh, S. W. et al. A mesoscale connectome of the mouse brain. *Nature* **508**, 207–214 (2014).
64. Buckner, R. L. & Krienen, F. M. The evolution of distributed association networks in the human brain. *Trends Cogn. Sci.* **17**, 648–665 (2013).
65. Petanjek, Z. et al. Extraordinary neoteny of synaptic spines in the human prefrontal cortex. *Proc. Natl Acad. Sci. USA* **108**, 13281–13286 (2011).
66. Kolb, B. et al. Experience and the developing prefrontal cortex. *Proc. Natl Acad. Sci. USA* **109**, 17186–17193 (2012).
67. Chini, M. & Hanganu-Opatz, I. L. Prefrontal cortex development in health and disease: lessons from rodents and humans. *Trends Neurosci.* **44**, 227–240 (2021).
68. Kolk, S. M. & Rakic, P. Development of prefrontal cortex. *Neuropsychopharmacology* **47**, 41–57 (2022).
69. Larivière, S. et al. Multiscale structure-function gradients in the neonatal connectome. *Cereb. Cortex* **30**, 47–58 (2019).
70. Ball, G. et al. Cortical morphology at birth reflects spatiotemporal patterns of gene expression in the fetal human brain. *PLoS Biol.* **18**, e3000976 (2020).
71. Nielsen, A. N. et al. Maturation of large-scale brain systems over the first month of life. *Cereb. Cortex* **33**, 2788–2803 (2022).
72. Larsen, B., Sydnor, V. J., Keller, A. S., Yeo, B. T. T. & Satterthwaite, T. D. A critical period plasticity framework for the sensorimotor-association axis of cortical neurodevelopment. *Trends Neurosci.* **46**, 847–862 (2023).
73. Freeman, W. J., Holmes, M. D., Burke, B. C. & Vanhatalo, S. Spatial spectra of scalp EEG and EMG from awake humans. *Clin. Neurophysiol.* **114**, 1053–1068 (2003).
74. Wallois, F. et al. Back to basics: the neuronal substrates and mechanisms that underlie the electroencephalogram in premature neonates. *Neurophysiol. Clin.* **51**, 5–33 (2021).
75. Vanhatalo, S. & Kaila, K. Development of neonatal EEG activity: from phenomenology to physiology. *Semin. Fetal Neonatal Med.* **11**, 471–478 (2006).
76. Vanhatalo, S. et al. Slow endogenous activity transients and developmental expression of K⁺-Cl⁻ cotransporter 2 in the immature human cortex. *Eur. J. Neurosci.* **22**, 2799–2804 (2005).
77. Yrjölä, P., Vanhatalo, S. & Tokariev, A. Neuronal coupling modes show differential development in the early cortical activity networks of human newborns. *J. Neurosci.* **44**, e1012232024 (2024).
78. Omidvarnia, A., Fransson, P., Metsäranta, M. & Vanhatalo, S. Functional bimodality in the brain networks of preterm and term human newborns. *Cereb. Cortex* **24**, 2657–2668 (2014).
79. Wallace, J. L. & Pollen, A. A. Human neuronal maturation comes of age: cellular mechanisms and species differences. *Nat. Rev. Neurosci.* **25**, 7–29 (2024).
80. Kostovic, I. & Judoš, M. Prolonged coexistence of transient and permanent circuitry elements in the developing cerebral cortex of fetuses and preterm infants. *Dev. Med. Child Neurol.* **48**, 388–393 (2006).
81. Linker, S. B. et al. Human-specific regulation of neural maturation identified by cross-primate transcriptomics. *Curr. Biol.* **32**, 4797–4807.e5 (2022).
82. Petanjek, Z., Banovac, I., Sedmak, D. & Hladnik, A. Dendritic spines: synaptogenesis and synaptic pruning for the developmental organization of brain circuits. *Adv. Neurobiol.* **34**, 143–221 (2023).
83. Wang, L. et al. A cross-species proteomic map reveals neoteny of human synapse development. *Nature* **622**, 112–119 (2023).
84. Schmidt Mellado, G. et al. The impact of premature extrauterine exposure on infants' stimulus-evoked brain activity across multiple sensory systems. *NeuroImage Clin.* **33**, 102914 (2021).
85. Witteveen, I. F. et al. Preterm birth accelerates the maturation of spontaneous and resting activity in the visual cortex. *Front. Integr. Neurosci.* **17**, 1149159 (2023).
86. Karolis, V. R. et al. Volumetric grey matter alterations in adolescents and adults born very preterm suggest accelerated brain maturation. *NeuroImage* **163**, 379–389 (2017).
87. Hedderich, D. M. et al. Increased brain age gap estimate (BrainAGE) in young adults after premature birth. *Front. Aging Neurosci.* **13**, 653365 (2021).
88. Padilla, N. et al. Breakdown of whole-brain dynamics in preterm-born children. *Cereb. Cortex* **30**, 1159–1170 (2020).
89. Yrjölä, P., Stjerna, S., Palva, J. M., Vanhatalo, S. & Tokariev, A. Phase-based cortical synchrony is affected by prematurity. *Cereb. Cortex* **32**, 2265–2276 (2022).
90. França, L. G. S. et al. Neonatal brain dynamic functional connectivity in term and preterm infants and its association with early childhood neurodevelopment. *Nat. Commun.* **15**, 16 (2024).
91. Noori, R. et al. Activity-dependent myelination: a glial mechanism of oscillatory self-organization in large-scale brain networks. *Proc. Natl Acad. Sci. USA* **117**, 13227–13237 (2020).
92. de Faria, J. O. et al. Periods of synchronized myelin changes shape brain function and plasticity. *Nat. Neurosci.* **24**, 1508–1521 (2021).
93. Back, S. A. White matter injury in the preterm infant: pathology and mechanisms. *Acta Neuropathol.* **134**, 331–349 (2017).
94. McNamara, N. B. & Miron, V. E. Microglia in developing white matter and perinatal brain injury. *Neurosci. Lett.* **714**, 134539 (2020).
95. Forbes, T. A. et al. Environmental enrichment ameliorates perinatal brain injury and promotes functional white matter recovery. *Nat. Commun.* **11**, 964 (2020).
96. Goldstein, E. Z., Pertsovskaya, V., Forbes, T. A., Dupree, J. L. & Gallo, V. Prolonged environmental enrichment promotes developmental myelination. *Front. Cell Dev. Biol.* **9**, 665409 (2021).
97. DeMaster, D. et al. Nurturing the preterm infant brain: leveraging neuroplasticity to improve neurobehavioral outcomes. *Pediatr. Res.* **85**, 166–175 (2019).
98. Puxeddu, M. G., Pope, M., Varley, T. F., Faskowitz, J. & Sporns, O. Leveraging multivariate information for community detection in functional brain networks. Preprint at <https://doi.org/10.1101/2024.07.22.604675> (2024).
99. Bossomaier, T., Barnett, L., Harré, M. & Lizier, J. T. *An Introduction to Transfer Entropy: Information Flow in Complex Systems* (Springer, 2016).
100. Kozachenko, L. F. & Leonenko, N. N. Sample estimate of the entropy of a \sim -random vector. *Probl. Inf. Transm.* **23**, 9 (1987).

101. Delattre, S. & Fournier, N. On the Kozachenko-Leonenko entropy estimator. *J. Stat. Plan. Inference* **185**, 69–93 (2017).
102. Kraskov, A., Stögbauer, H. & Grassberger, P. Estimating mutual information. *Phys. Rev. E* **69**, 066138 (2004).
103. Woodward, L. J., Ludwig, R. J., Gong, A., Myers, M. M. & Welch, M. G. Family Nurture Intervention and mother-preterm infant autonomic emotional connection in the neonatal intensive care unit: a review. *Acta Paediatr.* **114**, 760–771 (2025).
104. Welch, M. G. et al. Electroencephalographic activity of preterm infants is increased by Family Nurture Intervention: a randomized controlled trial in the NICU. *Clin. Neurophysiol.* **125**, 675–684 (2014).
105. Bourel-Ponchel, E., Hasaerts, D., Challamel, M.-J. & Lamblin, M.-D. Behavioral-state development and sleep-state differentiation during early ontogenesis. *Neurophysiol. Clin.* **51**, 89–98 (2021).
106. André, M. et al. Electroencephalography in premature and full-term infants. developmental features and glossary. *Neurophysiol. Clin.* **40**, 59–124 (2010).
107. Asayesh, A., Vanhatalo, S. & Tokariev, A. The impact of EEG electrode density on the mapping of cortical activity networks in infants. *NeuroImage* **303**, 120932 (2024).
108. Tokariev, A. et al. Preterm birth changes networks of newborn cortical activity. *Cereb. Cortex* **29**, 814–826 (2019).
109. Despotovic, I. et al. Relationship of eeg sources of neonatal seizures to acute perinatal brain lesions seen on MRI: a pilot study. *Hum. Brain Mapp.* **34**, 2402–17 (2013).
110. Odabae, M. et al. Neonatal eeg at scalp is focal and implies high skull conductivity in realistic neonatal head models. *Neuroimage* **96**, 73–80 (2014).
111. Tokariev, A., Vanhatalo, S. & Palva, J. M. Analysis of infant cortical synchrony is constrained by the number of recording electrodes and the recording montage. *Clin. Neurophysiol.* **127**, 310–23 (2016).
112. Gramfort, A., Papadopoulos, T., Olivi, E. & Clerc, M. Openmeeg: opensource software for quasistatic bioelectromagnetics. *Biomed. Eng. Online* **9**, 45 (2010).
113. Dale, A. M. et al. Dynamic statistical parametric mapping: combining fMRI and meg for high-resolution imaging of cortical activity. *Neuron* **26**, 55–67 (2000).
114. Tadel, F., Baillet, S., Mosher, J. C., Pantazis, D. & Leahy, R. M. Brainstorm: a user-friendly application for meg/eeg analysis. *Comput. Intell. Neurosci.* **2011**, 879716 (2011).
115. Johnson, S., Moore, T. & Marlow, N. Using the Bayley-III to assess neurodevelopmental delay: which cut-off should be used? *Pediatr. Res* **75**, 670–4 (2014).
116. Cover, T. M. & Thomas, J. A. *Elements of Information Theory* (John Wiley & Sons, 2012).
117. Rosas, F. E. et al. Disentangling high-order mechanisms and high-order behaviours in complex systems. *Nat. Phys.* **18**, 1–2 (2022).
118. Makkeh, A., Gutknecht, A. J. & Wibral, M. Introducing a differentiable measure of pointwise shared information. *Phys. Rev. E* **103**, 032149 (2021).
119. Varley, T. F. & Kaminski, P. Untangling synergistic effects of intersecting social identities with partial information decomposition. *Entropy* **24**, 1387 (2022).
120. Watanabe, S. Information theoretical analysis of multivariate correlation. *IBM J. Res. Dev.* **4**, 66–82 (1960).
121. Tononi, G., Sporns, O. & Edelman, G. M. A measure for brain complexity: relating functional segregation and integration in the nervous system. *Proc. Natl Acad. Sci. USA* **91**, 5033–5037 (1994).
122. Metropolis, N., Rosenbluth, A. W., Rosenbluth, M. N., Teller, A. H. & Teller, E. Equation of state calculations by fast computing machines. *J. Chem. Phys.* **21**, 1087–1092 (1953).
123. Smola, A. J. & Schölkopf, B. A tutorial on support vector regression. *Stat. Comput.* **14**, 199–222 (2004).
124. Stevenson, N. J. et al. Inter-site generalizability of eeg based age prediction algorithms in the preterm infant. *Physiol. Meas.* **44**, 07NT01 (2023).
125. Xia, M., Wang, J. & He, Y. BrainNet Viewer: a network visualization tool for human brain connectomics. *PLoS ONE* **8**, e68910 (2013).

Acknowledgements

This work was funded by The Finnish Academy (335778, 332017 to S.V. and 321235 to A.T.), the Sigrid Jusélius Foundation (P.Y., S.V., A.T.). T.F.V. was supported by NSF-NRT grant 1735095, Interdisciplinary Training in Complex Networks and Systems. P.Y. was supported by Päivikki and Sakari Sohlbergin Säätiö as well as by Orion Research Foundation. T.F.V. would like to thank Mrs. Maria Pope for her expertise on simulated annealing. Open access was funded by Helsinki University Library.

Author contributions

T.F.V., O.S., and A.T. conceived the project. M.G.W. and M.M.M. conceptualized interventions and coordinated data collection. P.Y., S.V., and A.T. curated EEG data. P.Y. pre-processed EEG data. T.F.V., O.S., N.J.S., and A.T. developed analytical tools. T.F.V., O.S., and A.T. analyzed data. A.T. created figures. T.F.V., O.S., S.V., and A.T. wrote the original manuscript. N.J.S., P.Y., M.G.W., and M.M.M. reviewed and edited the manuscript. A.T. supervised the project.

Competing interests

The authors declare no competing interests.

Additional information

Supplementary information The online version contains supplementary material available at <https://doi.org/10.1038/s42003-025-08082-z>.

Correspondence and requests for materials should be addressed to Anton Tokariev.

Peer review information *Communications Biology* thanks Daniel Bor, Rodrigo Cofre and the other, anonymous, reviewer(s) for their contribution to the peer review of this work. Primary Handling Editors: Enzo Tagliazucchi and Christina Karlsson Rosenthal.

Reprints and permissions information is available at <http://www.nature.com/reprints>

Publisher's note Springer Nature remains neutral with regard to jurisdictional claims in published maps and institutional affiliations.

Open Access This article is licensed under a Creative Commons Attribution-NonCommercial-NoDerivatives 4.0 International License, which permits any non-commercial use, sharing, distribution and reproduction in any medium or format, as long as you give appropriate credit to the original author(s) and the source, provide a link to the Creative Commons licence, and indicate if you modified the licensed material. You do not have permission under this licence to share adapted material derived from this article or parts of it. The images or other third party material in this article are included in the article's Creative Commons licence, unless indicated otherwise in a credit line to the material. If material is not included in the article's Creative Commons licence and your intended use is not permitted by statutory regulation or exceeds the permitted use, you will need to obtain permission directly from the copyright holder. To view a copy of this licence, visit <http://creativecommons.org/licenses/by-nc-nd/4.0/>.

© The Author(s) 2025